

The crossover from 2D to 3D percolation and its relationship to glass transition in thin films. Theory and numerical simulations

Paul Sotta and Didier Long
Laboratoire de Physique des Solides
Université de Paris XI, Bât. 510
91405 Orsay Cedex, France

(Dated: November 3, 2018)

We consider here the percolation problem in thin films, both in the direction normal to the film and in the direction parallel to the film. We thereby describe here the cross-over between 2D and 3D percolation, which we do on cubic and square lattices. The main relations are derived using scaling and real space renormalisation arguments. They are checked by numerical simulations, which also provide the numerical prefactors. We calculate in particular the correlation length parallel to the film, the average mass and the mass distribution $n(m)$ of the clusters. In particular, we show that the latter is given by a master function of $h^{-D+1/\sigma_2\nu_3}|p - p_c(h)|^{1/\sigma_2}m$, where h is the thickness of the film and D, ν_3, σ_2 are tabulated 2D and 3D critical exponents. $p_c(h)$ is the percolation threshold of the film which we also calculate. These results are of interest in particular for describing the glass transition in thin polymer films.

I. INTRODUCTION

The building of macroscopic continuous objects (aggregates, or clusters) by the random dispersion of particles (sites) or bonds has been the subject of many studies over the past decades, and has been formalised by various models of percolation [1, 2, 3, 4]. The corresponding issues are essential for determining important macroscopic properties such as the electric conductivity [1, 3], the visco-elastic behaviour [5] of various systems, or more generally mechanical properties [6]. For a review on the latter aspect, see e.g. [7]. The main quantities of interest have been expressed as power laws, close to a critical point, and the main results are summarised by a list of critical exponents, which do not depend on the details of the models but only on the spatial dimension. Due to the dependence of critical phenomena on spatial dimension, the cross-over between 2D and 3D behaviours has been the subject of various studies, e.g. in the case of magnetic phenomena [8], for describing the phase transition behavior of thin magnetic films for instance. For studying the conductivity of thin composite systems, Clerc et al considered the cross-over between 2D and 3D percolation and calculated the percolation threshold as a function of the thickness of the film, using finite scaling arguments [9]. This issue has also been considered by Vicsek and Kertész [10].

Another field where percolation appears to be a key concept is the glass transition in supercooled liquids. The most prominent feature of this phenomena is a dramatic increase of the viscosity when cooling such liquids. Though very steep, this increase is continuous and does not appear to involve a phase transition. For a review on the glass transition see e.g. [11, 12]. To account for experiments which have demonstrated the heterogeneous nature of the dynamics when approaching the glass transition [13, 14, 15, 16, 17] (see e.g. [18, 19, 20] for review),

it has been proposed recently [21, 22] that the glass transition corresponds to the percolation of domains with relaxation times larger or equal to the arbitrary time τ_g set for defining the glass transition. According to this model, the slow domains correspond to denser regions resulting from density fluctuations of Gaussian statistics. These slow domains, of typical size 2 to 4 nm, coexist with faster domains with relaxation times order of magnitude shorter [18, 19, 20, 21, 22]. This model, aimed at explaining experimental results regarding the heterogeneous nature of the dynamics close to the glass transition, allows also to explain the shift of the glass transition temperature T_g of thin polymer films, a few tens of nanometer thick. Indeed, it has been demonstrated over the past ten years that the dynamical behaviour of thin polymer films is very different from that of the same polymer in the bulk. It is now well established that films with weak interactions with their substrate (or freely suspended films) display a reduction of T_g , of about 20 K for films 10 nm thick [23, 24]. On the contrary films with strong interactions with their substrate display an increase of T_g by as much as 60K for films 10 nm thick [25, 26, 27]. For review of the corresponding issues see e.g. [28, 29]. In the model of Long and co-workers [21, 22, 30], these effects result from percolation mechanisms. According to this model, the glass transition is controlled by the percolation of small subunits of relaxation time τ_g . Therefore, the shifts in T_g in a film are closely related to the differences in the percolation properties in a film (i.e. in a system of small, finite thickness) with respect to a bulk system. In the case of a thin suspended film, percolating in the direction parallel to the film requires a larger fraction of these slow subunits, and thereby takes place at a temperature lower than the bulk T_g .

In the case of a strongly interacting film, the glass transition occurs when aggregates of slow subunits have a diameter comparable to the thickness of the film, due to different boundary conditions. As a consequence, in

both cases the glass transition corresponds to the temperature at which the correlation length of the 3D percolation problem is equal (or comparable) to the thickness of the film, in one case (weak interactions) above the 3D percolation threshold, and in the other one (strong interactions) below the 3D percolation threshold. In the case of intermediate interactions between the monomers and the substrate [31, 32], as described in [30], the glass transition corresponds to a lateral extension of a slow aggregate larger than the film thickness, and such that the number of monomers of this aggregate in contact with the substrate is large enough so that the time for this aggregate to desorb is equal to τ_g . Describing all these cases -weak interactions, strong interactions, intermediate interactions- requires thereby a precise understanding of the cross-over between 2D and 3D percolation [21, 22]. This is the aim of this paper. A better description of this cross-over should also be useful for describing the mechanical properties of films made of composite materials, or for the conductivity properties of thin films [1, 9].

The questions which we address here stem from our modeling of the glass transition in thin films. When considering a thin suspended film, we argued [21, 22] that the glass transition corresponds to the percolation in the direction parallel to the film. Then, we will consider this problem here, in films of dimensionless thickness h , expressed in units of the size $\xi \sim 2\text{-}4$ nm of the dynamical heterogeneities [15, 22]. Then, one of the questions is: what is the percolation threshold $p_c(h)$ knowing the 3D percolation threshold p_c^{3D} ? How does the lateral extension of the aggregates increase when approaching this threshold? When considering films strongly attached to their substrate, we argued that the glass transition corresponds to the appearance of a fraction of order 1 of monomers from one interface connected to the opposite interface by continuous path of slow subunits. We thus study the correlation function between sites on one interface and sites on the other, to determine precisely how the connected fraction evolves with the fraction p of occupied sites. Finally, to consider the crossover between these two regimes, we need to know the size of the aggregates, the number of monomers of one aggregate in contact with the interacting substrate, and the distribution of mass of the aggregates.

The present work is based on the idea that a system of finite thickness h may be renormalised to a 2D system, by changing the 2D percolation threshold p_c^{2D} into a renormalised value $p_c(h)$. A first step will be therefore to determine $p_c(h)$. We describe a real-space renormalisation procedure to transform the quasi-2D problem of a film of finite thickness into a 2D problem. This allows for calculating various quantities of interest, as a function of known 2D and 3D critical exponents and of a renormalised occupation probability. The corresponding results are exact at the level of scaling laws. To check these predictions, and to obtain the values of the pre-factors, we then perform numerical simulations. The paper is organized as follows. In section **II.A**, we introduce some

TABLE I: The values of the percolation thresholds in various cases

Lattice	Site	Bond
square (2D)	0.592746	0.50
simple cubic	0.3117	0.2492
FCC	0.198	0.119

classical definitions, notations and we recall some basic concepts and results regarding percolation theory, either in 2D or in 3D. Specifically we recall the various quantities which have a critical behaviour at the percolation threshold. In section **II.B**, we introduce some classical finite size scaling arguments regarding the definition of the percolation threshold on a finite system. Then in section **II.C**, we show how the percolation problem in a film of finite thickness can be mapped on a 2D system with a new percolation threshold $p_c(h)$. Various scaling laws are derived, regarding $p_c(h)$, the mass of the aggregates, the connectivity between both interfaces. In section **III** we describe the numerical Monte-Carlo algorithm used for our simulations. Finally in sections **IV**, **V** and **VI** we discuss the results of our numerical simulations, in connection with the various scaling laws derived in **II.C**.

II. BACKGROUND ON PERCOLATION

A. Critical behaviour at $p = p_c$

Let us recall some basics about 2D or 3D percolation which will be useful in the following. For a review of the definitions and results presented here see e.g. [1]. The control parameter in site percolation problems is the site occupation probability p . The percolation threshold is the critical value p_c at which an infinite cluster appears. The value p_c is not universal. It depends on the particular type of lattice which is considered. Values of the percolation thresholds in various cases are summarized in Table I. In the following, the various exponents are generically designed by greek letters. When some relations are valid only using a 2D or a 3D exponent, the corresponding exponents are written with a subscript 2 or 3 according to the dimension.

For the sake of definiteness and when it is necessary to be specific, we will consider in this paper percolation on cubic lattices (3D or in films), and on square lattices for 2D systems. Only the prefactors depend on this choice, the exponents of the various scaling laws that we derive do not. We call $n(m)$ the number of clusters of mass m (the mass m of a cluster is the number of sites which belong to it) per lattice site (i.e. the total number of clusters of size m divided by the volume of the system), at a given occupation probability p . The quantity $mn(m)$ therefore equals the probability for a given site to belong to a cluster of mass m . The occupation probability is thus $p = \sum m n(m)$. The distribution of cluster masses

is represented by a function of the form:

$$n(m) \approx m^{-\tau} f(m/m_\zeta) \quad (1)$$

where $f(m/m_\zeta)$ behaves like

$$f(m/m_\zeta) \approx e^{-m/m_\zeta} \quad (2)$$

for $m \gg m_\zeta$ and has a finite value at zero. For m smaller than the typical value m_ζ , the power law dominates. For m larger than m_ζ , the exponential dominates, which means that clusters with a mass larger than m_ζ are exponentially rare. m_ζ diverges at p_c with a critical exponent denoted by $1/\sigma$:

$$m_\zeta \approx |p - p_c|^{-1/\sigma} \quad (3)$$

In 2D, the exponent $\sigma_2 = 36/91 = 0.3956$ (or $1/\sigma_2 = 2.5278$) and the exponent $\tau_2 = 187/91 = 2.055$ (see Table I).

On the other hand, a mean cluster mass may be defined for $p < p_c$ as the second moment:

$$M = \frac{\sum m^2 n(m)}{\sum m n(m)} \quad (4)$$

The mean cluster mass M diverges at the threshold $p = p_c$ with another exponent γ :

$$M \approx |p - p_c|^{-\gamma} \quad (5)$$

In 2D: $\gamma_2 = 43/18 = 2.389$.

Since $\sum m n(m) \equiv p$ (or equivalently, since $\tau > 2$), the divergence is contained in the numerator in eq. (4), which reads:

$$M \approx \int m^{2-\tau} f\left(\frac{m}{m_\zeta}\right) dm \propto m_\zeta^{3-\tau} \quad (6)$$

Note that M grows with $|p - p_c|$ more slowly than m_ζ . This is because M is an average mass (second moment of the cluster number $n(m)$), whereas m_ζ is the cut-off mass of the distribution. Combining eq. (3), (5) and (6), one finds:

$$\gamma = \frac{3 - \tau}{\sigma} \quad (7)$$

Note that, at $p = p_c$, the distribution $n(m)$ reduces to $n(m) \approx m^{-\tau}$.

We consider now the spatial extension of the clusters. One can define the correlation function (or connectivity function) $g(r)$ as the probability that a site at the distance r from an occupied site is also occupied and belongs to the same cluster. The correlation length may be defined from $g(r)$ as:

$$\zeta^2 = \frac{\sum_r r^2 g(r)}{\sum_r g(r)} \quad (8)$$

For $p < p_c$, $g(r)$ is represented by a function of the form:

$$g(r) \approx r^{-(d-2+\eta)} G(r/\zeta) \quad (9)$$

where d denotes the dimensionality of space, and η is the anomalous exponent of the correlation function [1]. For $r \ll \zeta$, the power law dominates. This means that at short scale, the system is insensitive to the presence of a cut-off length at a larger scale. At large scale ($r \gg \zeta$), the function G decays exponentially $G(r/\zeta) \approx \exp(-r/\zeta)$. The correlation length ζ , which is proportional to some typical cluster diameter, diverges at the threshold as:

$$\zeta \approx |p - p_c|^{-\nu} \quad (10)$$

where, in 2D: $\nu_2 = 4/3$, and in 3D: $\nu_3 \approx 0.88$.

The radius of a cluster of mass m may be defined as:

$$2R_m^2 = \sum \frac{|r_{ij}|^2}{m^2} \quad (11)$$

where $|r_{ij}|^2$ is the squared distance between two occupied sites which belong to the same cluster of mass m , and where the sum is then averaged over all clusters of mass m . According to the definitions, it is easy to check that one has:

$$\zeta^2 = \frac{\sum R_m^2 m^2 n(m)}{\sum m^2 n(m)} \quad (12)$$

The correlation function $g(r)$ is related to the structure of the clusters, i.e. to the distribution of the mass inside a cluster. In 3-D, let us draw a volume of size h (of volume h^3) within a large cluster, such that h is small with respect to ζ . The number of sites within this volume which belong to this cluster is:

$$m = \int_0^h g(r) r^2 dr \quad (13)$$

And for $h < \zeta$:

$$m = \int_0^h r^{1-\eta} dr \approx h^{2-\eta} \quad (14)$$

In 3D, the exponent η is relatively small: $\eta = -0.068$. Setting $h = \zeta$ in eq. (14), one obtains the average mass M , as defined in eq. (5): $M \approx \zeta^{2-\eta}$, which gives another relation between critical exponents:

$$(2 - \eta)\nu = \gamma \quad (15)$$

We consider now the distribution of radius of the clusters for $p \leq p_c$. The radius R_m of a cluster is related to its mass m by a scaling law:

$$m \approx R_m^D \quad (16)$$

However, the exponent (or apparent exponent) D is not the same below, at and above p_c [1]. For $p = p_c$, the 3D critical exponent is $D_3 \approx 2.53$, and for $p < p_c$, the scaling relation, i.e. the fractal exponent, depends on the considered radius. Thus, more generally, it is assumed that the relation between the mass and the spatial extension is of the form [1]:

$$R_m \approx m^{1/D} f[(p - p_c)m^\sigma] \quad (17)$$

TABLE II: The values of some of the critical exponents, which will be used in the following

Exponent	$d = 2$	$d = 3$
τ	187/91=2.055	2.18
σ	36/91=0.3956	0.45
γ	43/18=2.389	1.80
ν	4/3	0.88
$1/D(p = p_c)$	49/91=0.5275	1/2.53=0.3952
$D(p < p_c)$	1.56	2
η	0.2084	-0.068

where the function f has to be determined numerically and satisfies the following properties: as $m \ll m_\zeta \approx |p - p_c|^{-1/\sigma}$ (where m_ζ has been defined in eq. (3)), i.e. as $x = |p - p_c|m^\sigma \ll 1$, $f(x)$ approaches a constant value. For $x \gg 1$, $f(x) \sim x^{1/D' - 1/D}$, where D' is the fractal exponent of large clusters for $p < p_c$. Away from p_c , $m_\zeta \approx |p - p_c|^{-1/\sigma}$ is finite, and defines a crossover from the behaviour $R_m \approx m^{1/D}$ for $m < m_\zeta$ to another power law $R_m \approx m^{1/D'}$ for $m > m_\zeta$. At p_c , m_ζ diverges. The exponent $1/D$ in eq. (17) is therefore the one which is measured at p_c (or very close to p_c). This exponent takes the values $1/D_3 = 1/2.53 = 0.39526$ in 3D and $1/D_2 = 48/91 = 0.5275$ in 2D. For clusters with a mass larger than m_ζ , at $p < p_c$, the value of the fractal exponent is smaller: $D_3 = 2$. This means that for $p < p_c$, large clusters are more tenuous than small ones, while they are self-similar whatever the size at p_c . The above discussion means that the crossover takes place on a spatial scale ζ . For small clusters with $R_m < \zeta$ (or for small masses $m < m_\zeta$), the value of the critical exponent is that at $p = p_c$ ($D \approx 2.53$ in 3D), and for larger clusters the exponent is that at $p < p_c$ ($D = 2$ in 3D). The cross-over between these two behaviours takes place at $R_m = \zeta$, corresponding to the mass $m_\zeta = \zeta^D$, where D is the critical exponent at p_c . Note that the cross-over goes to larger scales when p tends to p_c and there is a single exponent at p_c . All this means that at short scales (i.e. at scales significantly shorter than the correlation length ζ), the system does not know whether it percolates at larger scales or not.

Combining eqs. (3), (10) and (16), one gets another relation between critical exponents:

$$\frac{1}{\sigma} = \nu D \quad (18)$$

where D has the value at $p = p_c$ here.

B. Percolation in a finite system

The problem in numerical simulations is: how to extract the value of the percolation threshold (which is defined at infinite size) from simulations done in boxes of finite size? Percolation in a system of size L is defined by

the appearance of one cluster of radius L . The probability that a system of linear size L (volume L^3) percolates at an occupation probability p is of the form:

$$\Phi_L(p) \approx f(L(p_c - p)^\nu) \quad (19)$$

where the exponent ν has been introduced in eq. (10). Eq. (19) means that the probability to percolate in a system of size L is identical to the probability of appearance of a cluster of radius L in an infinite system, or, equivalently, that a system of size L percolates when the correlation length $\zeta(p) = L$ (where ζ is defined e.g. in eq. (10)). According to eq. (19), the curves $\Phi_L(p)$ become steeper as L increases. We call $p_c(L)$ the occupation probability corresponding to a given probability to percolate P . It follows from eq. (19) that in a system of size L , $p_c(L)$ varies as:

$$|p_c(L) - p_c| \approx L^{-1/\nu} \quad (20)$$

Eq. (20) will be used in the following to determine percolation thresholds p_c (extrapolated at infinite size) from simulations in boxes of various finite sizes. The percolation threshold $p_c(n)$ will be given by the number giving the best regression with exponent $-1/\nu$ (according to eq. (20)).

C. Rescaling a system of finite thickness h

Consider a thin film with mesh size unity, probability of site occupation p and of thickness h . The probability of occupation p may be larger or smaller than p_c^{3D} and is such that the corresponding 3D correlation length ζ_{3D} is larger than the thickness h of the film, that is:

$$p_c^-(h) \lesssim p \lesssim p_c^+(h) \quad (21)$$

The quantities $p_c^+(h)$ and $p_c^-(h)$ correspond to a correlation length for the 3D percolation problem comparable to the thickness of the film. p_c^- is smaller than the 3D percolation threshold p_c^{3D} , and p_c^+ is larger than p_c^{3D} . We aim now at calculating the percolation threshold of the film, $p_c(h)$. Note that we consider here percolation in the direction parallel to the film. By a coarse graining procedure, this problem can be transformed into a 2D problem. The corresponding coarse graining function is denoted by Φ . After one iteration, the probability of occupation is transformed into $\Phi(p)$. p_c^{3D} is the fixed point of Φ . Let us define $\kappa > 1$ as the scale factor of the renormalisation procedure. N is a number such that

$$\kappa^N = h \quad (22)$$

which means that the film is transformed into a 2D squared lattice after N iterations. If the initial film is at the percolation threshold, one requires that after these N iterations the film is transformed into a 2D lattice close to the 2D percolation threshold, that is $p = p_c(h)$ is transformed into $\Phi^N(p_c(h))$ such that

$$\Phi^{(N)}(p_c(h)) - p_c^{3D} \sim p_c^{2D} - p_c^{3D} \quad (23)$$

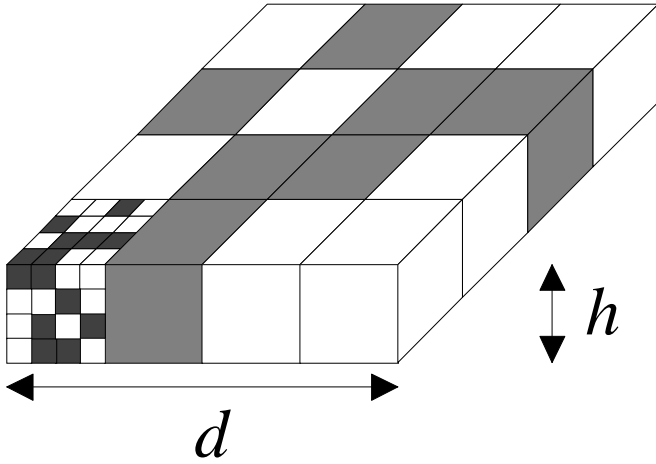


FIG. 1: Schematics illustrating the renormalization of the percolation problem in a film of thickness h to a two dimensional system.

One has then

$$\lambda^N(p_c(h) - p_c^{3D}) = \alpha \quad (24)$$

where α is a positive number comparable to $p_c^{2D} - p_c^{3D}$ and where

$$\lambda = \frac{d\Phi}{dp}(p = p_c^{3D}) \quad (25)$$

Therefore

$$p_c(h) \approx p_c^{3D} + \alpha\lambda^{-N} \approx p_c^{3D} + \alpha h^{-1/\nu_3} \quad (26)$$

where ν_3 is the 3D critical exponent for the correlation length, which satisfies the relation:

$$\nu_3 = \frac{\log \kappa}{\log \lambda} \quad (27)$$

Note that the film percolation threshold $p_c(h)$ is larger than p_c^{3D} -percolating in thin films is more difficult than in the bulk- and that at $p_c(h)$ the 3D correlation length is comparable to h . In the following we take $p_c^+(h) = p_c(h)$. Let us consider now a situation where the probability of site occupation in the film is $p < p_c(h)$. By the same argument, p is transformed into $\Phi^{(N)}(p)$ with

$$\Phi^{(N)}(p) - p_c^{3D} \approx \lambda^N(p - p_c^{3D}) \quad (28)$$

This procedure is illustrated in Fig. 1. One has then

$$\Phi^{(N)}(p_c(h)) - \Phi^{(N)}(p) \approx \lambda^N(p_c(h) - p) \approx h^{1/\nu_3}(p_c(h) - p) \quad (29)$$

The quasi-2D problem of the film with probability of occupation p on a lattice of mesh size unity is then mapped on a 2D lattice with probability of occupation $\Phi^{(N)}(p)$ and mesh size h . The average mass $M'(h)$ of the aggregates, expressed in numbers of supersites of size h , is

therefore:

$$M'(h) \approx M'_0 |\Phi^{(N)}(p_c(h)) - \Phi^{(N)}(p)|^{-\gamma_2} \quad (30)$$

$$\approx M'_0 \left(h^{1/\nu_3} |p - p_c(h)| \right)^{-\gamma_2} \quad (31)$$

where M'_0 is a prefactor of order unity. Note that the above result insures that for $p = p_c^-(h)$, i.e. when the 3D correlation length is equal to the thickness of the film, the typical mass of the aggregates on the scale h is of order one as it should be. Note indeed that $p_c^-(h)$ is given by a relation

$$p_c^-(h) = p_c^{3D} - \alpha' h^{-1/\nu_3} \quad (32)$$

where α' is a positive number of order 1. Let us study now the structure of the clusters in the film, below but close to the percolation threshold $p_c(h)$, more precisely in the situation $h \ll \zeta_{3D}$. In this case, the lateral extension of the dominating cluster is large with respect to h . The 2D correlation length is, expressed in the equivalent renormalised 2D system:

$$\zeta'_{\parallel} \approx |\Phi^{(N)}(p) - p_c^{2D}|^{-\nu_2} \approx \left(h^{1/\nu_3} |p - p_c(h)| \right)^{-\nu_2} \quad (33)$$

Coming back to the original system, in units of elementary sites:

$$\zeta_{\parallel} \approx h \left(h^{1/\nu_3} |p - p_c(h)| \right)^{-\nu_2} \quad (34)$$

Here ζ_{\parallel} is the correlation length in the direction parallel to the film and provides the dominant lateral extension of the clusters. Of course this result is meaningful only when the occupation probability p is such that the 3D correlation length is larger than the thickness of the film. In units of the elementary sites of the initial film, M'_0 should then be replaced by the average mass within a h -cube. This is done using eq. (14): $M'_0 = M_0 h^{2-\eta}$ (because in all the interval studied here $h < \zeta_{3D}$). M_0 is a number of order unity. Finally, the average mass per cluster is, in units of elementary sites:

$$M \approx M_0 h^{2-\eta_3} \left(h^{1/\nu_3} |p - p_c(h)| \right)^{-\gamma_2} \quad (35)$$

Let us consider now the distribution of clusters $n(m)$. It obeys a scaling relation similar to eq. (17) (see also eq. (1)). In the equivalent renormalised 2D system, the number of clusters of mass m' (in units of h -cubes) is (see eqs. (1) and (3)):

$$n(m') \approx m'^{-\tau_2} g_2 \left(\frac{m'}{m'_{\zeta}} \right) \quad (36)$$

with:

$$m'_{\zeta} \approx |\Phi^{(N)}(p) - p_c^{2D}|^{-1/\sigma_2} \approx h^{-1/\nu_3 \sigma_2} |p - p_c(h)|^{-1/\sigma_2} \quad (37)$$

g_2 is the 2D function as defined by equation (1), and has to be determined numerically. $\tau_2 = 187/91 = 2.055$ and $1/\sigma_2 = 91/36 = 2.5278$ are the 2D values of the exponents (see Table I). The expressions for the masses M' and M can be obtained in a different way as that used above, which we consider now. From the mass distribution $n(m')$, one deduces the relation

$$M' \approx m_\zeta^{i3-\tau_2} \quad (38)$$

Using the same argument as that used to obtain equation (35), one obtains

$$M \approx h^{2-\eta_3} m_\zeta^{i3-\tau_2} \quad (39)$$

Then, from equation (37), the average mass M' on scale h can be written as

$$M' \approx h^{-(3-\tau_2)/(\nu_3\sigma_2)} |p - p_c(h)|^{-(3-\tau_2)/\sigma_2} \quad (40)$$

Finally, using the relation $(3 - \tau_2)/\sigma_2 = \gamma_2$, one recovers

$$M' \approx h^{-\gamma_2/\nu_3} |p - p_c(h)|^{-\gamma_2} \quad (41)$$

which is equation (31). To come back to the original film of thickness h , we need now to obtain the distribution $n(m)$ of the mass m of the aggregates on the scale of elementary sites. When the system is rescaled by a factor κ (in 3D), the correlation length is rescaled as $\zeta \rightarrow \frac{\zeta}{\kappa}$. Since the relation $m_\zeta = \zeta^{-1/(\sigma\nu)}$ must be preserved, m_ζ is thus rescaled as:

$$m_\zeta \rightarrow \frac{m_\zeta}{\lambda^{1/(\sigma_3\nu_3)}} \quad (42)$$

With $1/(\sigma\nu) = D$ (see eq. (18)), this leads to the rescaling $m_\zeta = h^{D_3} m'_\zeta$, where D_3 is here the 3D value of the exponent at $p = p_c$. Thus, we have to consider a scaling relation of the type:

$$n(m) \approx h^\omega m^{-\tau_2} g_{2D} \left[h^{-D_3+1/(\sigma_2\nu_3)} |p - p_c(h)|^{1/\sigma_2} m \right] \quad (43)$$

or equivalently

$$n(m) \approx h^\omega m^{-\tau_2} g_{2D} \left(h^{-D_3} \frac{m}{m'_\zeta} \right) \quad (44)$$

where ω can be determined by writing:

$$M = \int m^2 n(m) dm \approx h^{\omega+D_3(3-\tau_2)} m_\zeta^{i3-\tau_2} \quad (45)$$

Comparing with eq. (39), one obtains the equation $\omega + D_3(3 - \tau_2) = 2 - \eta_3$. Thereby the distribution of cluster masses is expected to be described by equation (43) or equation (44), the value of the exponent ω being given by

$$\omega = 2 - \eta_3 - D_3(3 - \tau_2) \quad (46)$$

Thus, the quantity $h^{-\omega} m^{\tau_2} n(m)$ should give a master curve when plotted versus the quantity $h^{-D_3+1/(\sigma_2\nu_3)} |p - p_c(h)|^{1/\sigma_2} m$. The exponent ω has the value $\omega = -0.323$. In the following, we consider numerical simulations regarding the relations derived in this section.

III. DESCRIPTION OF THE SYSTEM AND THE ALGORITHM

We compute the site percolation threshold in a square (2D) or simple cubic (3D) lattice of variable linear dimensions. Unit sites are occupied at random with a probability p . An improved random number generator (uniform deviate provided in numerical recipes in Fortran), is used, which, thanks to a shuffling procedure of the output, is known to provide perfect random numbers, within the limits of the floating point precision. Indeed, the random generator has to be called a number of times equal to the volume of the system times the number of sample systems used to average the data (that is, at most a few 10^{11}), which precludes the use of a standard, low quality random number generator.

The algorithm used to determine percolation thresholds is itself based on a renormalization procedure, which is either two- or three-dimensional. For instance, at a given step in the 3D procedure, d -cubes of linear size $d = 2^m$ (of volume $V = d^3$) are generated. The faces of the cube are occupied by atoms belonging to various clusters. Then, 8 such d -cubes are gathered to form one cube of linear size $2d = 2^{m+1}$ (volume $8V$), in which the clusters from all 8 elementary cubes are connected together and re-numbered. A Hoshen-Kopelman algorithm is used to renumber the clusters [33]. Then only the new clusters connected to one external face of the new cube at least are considered for the next step. The initial step consists in connecting together 8 unit sites of the lattice. Iterating the 3D procedure m times gives a system (a cube) of size 2^m . Then, a film of thickness h and lateral dimension $d = h^p$ may be generated by iterating p times a 2D procedure similar to the 3D one. The system percolates when there exists at least one cluster connecting the 6 external faces. The probability to percolate $P(p)$ is averaged over a number of different configurations (typically 50 to 500). Using the renormalization procedure, the curves $P(p)$ for all values of d (of the form $d = 2^j$) are obtained in a single run. Simulations were run on Pentium IV Personal Computers operating at 1.4 GHz with 512 Mo RAM or on a DecAlpha Work Station.

The algorithm was validated by studying the well-known cases of 2D (resp. 3D) square (resp. simple cubic) systems, in order to verify that percolation thresholds are obtained with a satisfactory precision. The probability to percolate P is measured as a function of the occupation probability p . In two dimensions, the curves $P(p)$ obtained for various sizes of the system (from $d = 2^3 = 8$ to $d = 2^{16} = 65536$, which corresponds to a surface d^2 from 64 to 4.295×10^9) become steeper when d increases, in agreement with eq. (19). We find here that all curves intersect at a fixed point which corresponds to an occupation probability $p_c^{2D} \approx 0.5927$ and a probability to percolate $P(p) \approx 0.327$. The value p_c is in agreement with that given in [1]. The curves $P(p)$ are well fitted (at least in the vicinity of the percolation threshold) by

a function of the form:

$$P(p) = \frac{1}{2} \left(1 + \tanh \left(\frac{p - p_c(d)}{q(d)} \right) \right) \quad (47)$$

in which both adjustable parameters $p_c(d)$ and $q(d)$ depend on the size d of the system. The form of this function is purely heuristic, as it merely provides an unambiguous way to extract the value of the threshold for each value of d . When the quantity $\log(p_c(d) - p_c^{2D})$ is plotted as a function of $\log d$, a straight line with a slope -0.75 ± 0.01 is obtained. This is in concordance with eq. (20), with the theoretical value $-1/\nu_2 = -3/4$. The quantity $q(d)$, plotted as a function of d in logarithmic scale does also give the power law behaviour $q(d) \approx d^{-1/\nu_2}$, in agreement with eq. (19). In 3D as well as in 2D, the curves $P(p)$ obtained for various sizes of the system (from $d = 8$ to $d = 2^9 = 512$, i.e. a volume 512 to 1.342×10^8) strongly depend on d . All curves intersect at the fixed point $p_c^{3D} = 0.3117$ and a probability to percolate $P(p) \approx 0.073$. The value p_c^{3D} is in agreement with that given in [1]. The curves $P(p)$ are fitted by a function of the same form as in the 2D case (eq. (47)). In 3D as well, the quantity $p_c(d) - p_c^{3D}$ varies as d^{-1/ν_3} , with the expected 3D value of the exponent $1/\nu_3 = 1/0.88 = 1.1364$. Note that the prefactor in this curve (as well as in the 2D curve) is arbitrary, as it depends on the probability level P at which $p_c(d)$ is measured. The scaling behaviour $q(d) \approx d^{-1/\nu_3}$ is well verified in this case also, in accordance with eq. (19).

IV. PERCOLATION THRESHOLD IN THE DIRECTION PARALLEL TO A FILM OF THICKNESS h

We consider the variation of the percolation threshold in a system of dimensions $d \times d \times h$ as a function of the thickness h of the system. Note that the corresponding results are of interest for calculating the negative shift of T_g in a freely suspended films [21, 30]. The thickness h was varied from $h = 1$ (which corresponds to the 2D system) to $h = 128$. For each value of h , the dimension d was varied from $d = h$ to $d = 1024$. The algorithm combines 3D renormalization up to a cube of dimensions $h \times h \times h$, then 2D renormalization of h -cubes up to a system of dimensions $d \times d \times h$. Percolation is defined here when one cluster at least connects all 6 external faces of the volume $d \times d \times h$ (see Fig. 2). For each couple of values (d, h) , the probability to percolate P is measured as a function of the occupation probability p . Some examples of the curves $P(p)$ are shown in Fig. 3. For each value of h , the curves corresponding to different values of d intersect at a fixed point, which may be considered as the percolation threshold $p_c(h)$. The curves are fitted by the same heuristic function as before, with two adjustable parameters $p_c(d, h)$ and $q(d, h)$:

$$P(p) = \frac{1}{2} \left(1 + \tanh \left(\frac{p - p_c(d, h)}{q(d, h)} \right) \right) \quad (48)$$

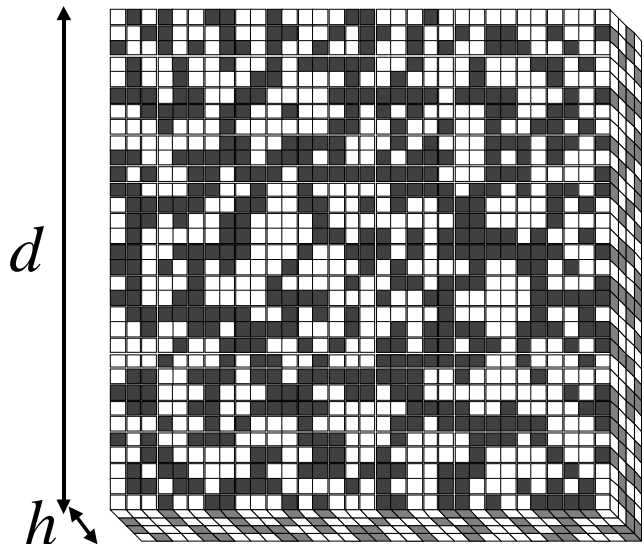


FIG. 2: Percolation in a system of dimensions $d \times d \times h$: there is a cluster spanning the whole surface of the system. This figure illustrates the case of a non-adsorbing film.

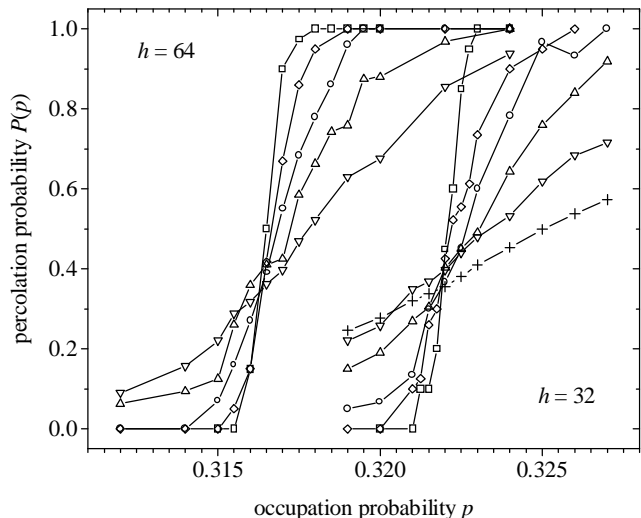


FIG. 3: The probability to percolate P as a function of the occupation probability p , obtained in systems of thickness h ($h = 32$ and $h = 64$) and lateral extension d : \square : $d = 1024$, \diamond : $d = 512$, \circ : $d = 256$, \triangle : $d = 128$, ∇ : $d = 64$, $+$: $d = 32$. For each value of h , the curves $P(p)$ become steeper as d increases and intersect at a fixed point $p_c(h)$.

The number value giving the best linear regression $p_c(d, h) - p_c(h) \approx d^{-1/\nu_2}$ (h being fixed), with the 2D value of the exponent $\nu_2 = 4/3$, will be adopted for the percolation threshold $p_c(h)$ in a film of thickness h , in the limit $d \rightarrow \infty$. Within error bars, this value $p_c(h)$ coincides with the fixed point mentioned above in the ensemble of curves $P(p)$. Thus, for a given thickness h and varying lateral size d , the following variation is ob-

TABLE III: The values of the percolation thresholds in a film of thickness h

h	$p_c(h)$
2	0.47424
4	0.3997
8	0.3557
16	0.3329
32	0.3219
64	0.3165

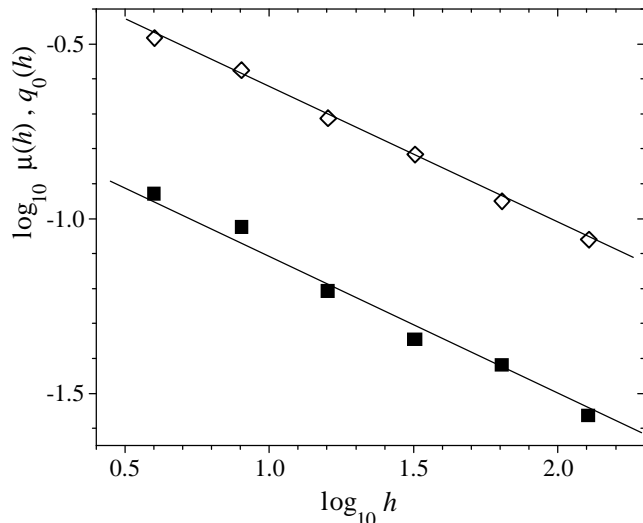


FIG. 4: ■ : the prefactor $\mu(h)$ in the curves $p_c(h, d) - p_c(h)$ versus d , as a function of h , \diamond : the prefactor $q_0(h)$ in the adjustable parameter $q(d, h)$, in logarithmic scale. The straight lines show the predicted behaviour $\mu(h), q_0(h) \propto h^{-0.386}$.

served:

$$p_c(d, h) - p_c(h) \approx \mu(h)d^{-1/\nu_2} \quad (49)$$

with $\nu_2 = 4/3$. The values obtained for the percolation thresholds $p_c(h)$ in a film of thickness h are summarized in Table III. The variation of the prefactor $\mu(h)$ may be estimated as follows. The 3D behaviour (up to the size h) gives $p_c(d) - p_c^{3D} = Ad^{-1/\nu_3}$ (see eq. (20)). Thus, setting $d = h$ in eq. (49):

$$p_c(h) + \mu(h)h^{-1/\nu_2} \approx p_c^{3D} + Ah^{-1/\nu_3} \quad (50)$$

which gives, since $p_c^{3D} - p_c(h) \approx h^{-1/\nu_3}$:

$$\mu(h) \approx h^{1/\nu_2 - 1/\nu_3} \quad (51)$$

The curve $\mu(h)$ is shown in Fig. 4. The variation is compatible with the exponent $1/\nu_2 - 1/\nu_3 = -0.386$. Note that the prefactor in eq. (51) is arbitrary, since it depends on the probability level P which is adopted to define percolation.

The same argument may be used to study the variation of the fitting parameter $q(d, h)$. It is indeed observed

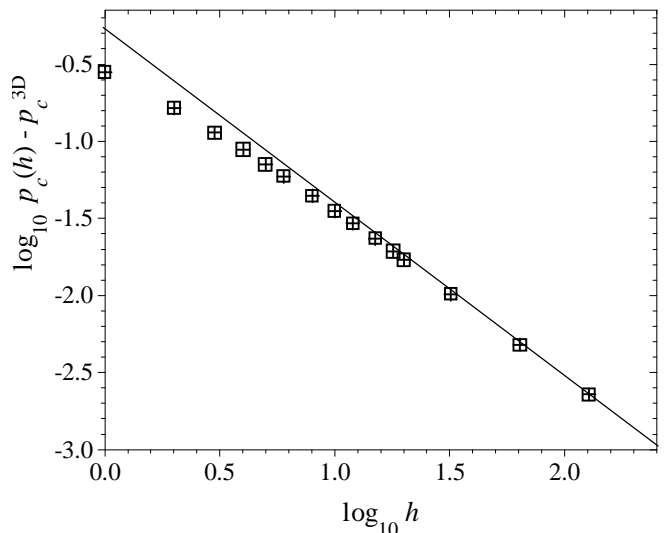


FIG. 5: The reduced percolation threshold $p_c(h) - p_c^{3D}$ as a function of the thickness h of the system, in logarithmic scale. The straight line represents the scaling law with the 3D exponent $-1/\nu_3 = -1.1364$. The scaling law is observed asymptotically.

that, varying d for a fixed value of h , a 2D scaling behaviour is observed: $q(d, h) = q_0(h)d^{-1/\nu_2}$ (see Fig. 4). The prefactor is observed to vary as $q_0(h) = q_0 h^{-0.386}$, in accordance with the expected variation, which may be inferred by exactly the same argument as was used for $\mu(h)$ (eq. (51)). The prefactor q_0 is not arbitrary here: it has the value 0.565. In Fig. 5, the percolation threshold $p_c(h) - p_c^{3D}$ is plotted as a function of h in logarithmic scale. The best linear fit has a slope -1.1364 which corresponds to the 3D value $1/\nu_3 = 1/0.88$ of the exponent, in agreement with eq. (26). Thus, in the asymptotic limit, the curve $p_c(h)$ writes :

$$p_c(h) - p_c^{3D} \approx \alpha h^{-1.138} \quad (52)$$

From Fig. 5, the prefactor α has the value $\alpha \approx 0.45$. Note that this value is of the same order as, but different from the value $p_c^{2D} - p_c^{3D} = 0.281$ (cf eq. (23)).

V. CORRELATION FUNCTION BETWEEN BOTH INTERFACES OF A FILM OF THICKNESS h

We consider here the correlation function between both interfaces of a thin film. The regime of interest here is that of a thickness h larger than the 3D correlation length of the percolation problem. Note that the corresponding results are of interest for calculating the positive shift of T_g in a strongly adsorbed film [21, 30]. Indeed, in the case of a strongly interacting film, the glass transition is related to the presence of *one* percolating cluster connecting the upper surface to the lower one (see Fig. 6). In the sense of percolation, glass transition will thus occur

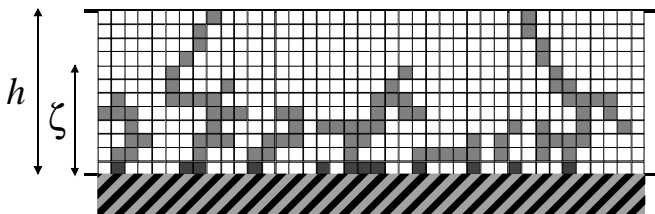


FIG. 6: Schematics of a film of thickness h in the regime $\zeta < h$. Only percolation clusters connected to the lower surface (i.e. to the substrate) are shown. Very few clusters reach the upper surface.

in this case, as soon as the 3D correlation length ζ becomes of the order of (still being smaller than) of h . The effective percolation threshold defined in this way is thus shifted downwards with respect to p_c^{3D} (since p_c^{3D} corresponds to $\zeta \rightarrow \infty$). Let us consider the average number of sites to which an occupied site of a given interface is connected to the other interface. This number $n_c(h)$ can be calculated by integrating the (3D) correlation function, expressed in eq. (9):

$$\begin{aligned} n_c(h) &\approx \int_0^\infty (r^2 + h^2)^{-\frac{1+\eta_3}{2}} e^{-\frac{(r^2+h^2)^{1/2}}{\zeta}} r dr \\ &= \int_h^\infty \rho^{-\eta_3} e^{-\frac{\rho}{\zeta}} d\rho \end{aligned} \quad (53)$$

Integrating by parts, this gives:

$$n_c(h) \approx h^{-\eta_3} \zeta e^{-\frac{h}{\zeta}} - \eta_3 \zeta \int_h^\infty \rho^{-1-\eta_3} e^{-\frac{\rho}{\zeta}} d\rho \quad (54)$$

The second term is negligible for $h \gg \zeta$.

In our simulations we have calculated the number $n_s(h)$ of sites of one interface which are connected to the other interface with at least one site. We expect a similar dependence of $n_c(h)$ as that given for $n_s(h)$ by equation eq. (54). In our simulations, we consider a system of dimension $d \times d \times h$ (with d large with respect to h). For a given value of the occupation probability p such that $\zeta < h$, we compute the number $n_s(h)$. The value of d is $d = 1024$, h ranges from $h = 1$ to $h = 64$. The algorithm makes use of a 1D renormalisation procedure : 2D slices of size $d \times d$ are generated and then glued together recursively, leading to systems of thickness 2, then 2^2 , etc, up to $2^6 = 64$.

For a given value of the occupation probability p (with $p < p_c^{3D}$), the quantity $\log n_s(h)$ exhibits a linear behaviour in the limit of large h values. Each curve was fitted with the first term in eq. (54), with two independent adjustable parameters η_3 and ζ . The values obtained for ζ in this way differ by less than 15% from those obtained by simply taking the slope of the asymptotic linear variation at large h values, i.e. by neglecting the influence of the $h^{-\eta_3}$ factor (remember that the exponent η is quite small). This difference is systematic and does not alter the variation as a function of $p_c^{3D} - p$ as it is shown in Fig. 7.

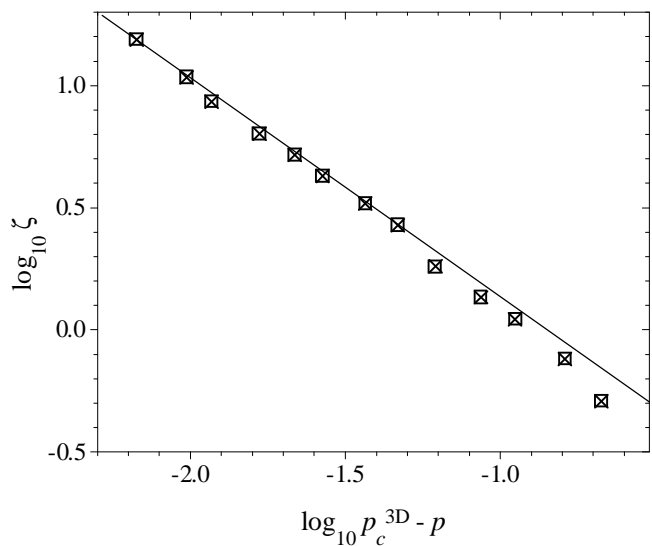


FIG. 7: The correlation length $\zeta(p)$ obtained from a linear fit of the curves $n_s(h)$ at large h values (see eq. (54)), versus $p_c^{3D} - p$, in logarithmic scale (p_c^{3D} is the 3D percolation threshold $p_c^{3D} = 0.3117$).

In Fig. 7, the correlation length $\zeta(p)$ is plotted as a function of $p_c^{3D} - p$, in logarithmic scale. The data are compared to a straight line of slope $-\nu_3 = -0.88$, which is the behaviour expected in the limit $p \rightarrow p_c$. An excellent agreement is obtained in the asymptotic limit. Thus we have:

$$\zeta(p) \approx \zeta_0 (p_c^{3D} - p)^{-\nu_3} \quad (55)$$

with $\zeta_0 \approx 0.185$. Note that two opposite requirements have to be reconciled in this section: observing the critical power law $\zeta(p) \approx (p_c - p)^{-\nu_3}$ urges for coming close enough to p_c^{3D} , while maintaining ζ small enough to make the regime $h > \zeta$ observable.

VI. CLUSTER NUMBER IN A FILM OF THICKNESS h

The regime of interest here corresponds to a 3D correlation length larger than the thickness of the film, either below the 3D percolation threshold, or above. The diagram in Fig. 8 summarizes the results obtained so far. p is the occupation probability, h the film thickness (that is, the number of slices in the simulated system). The curve $p_c^-(h)$ is defined as the ensemble of points where the measured 3D correlation length ζ is equal to h . Note that this curve corresponds to the percolation threshold associated to glass transition in a strongly adsorbed film, as it was defined in Section V. According to eq. 55, it is described by the equation:

$$p_c^{3D} - p = \left(\frac{h}{\zeta_0} \right)^{-1/\nu_3} \quad (56)$$

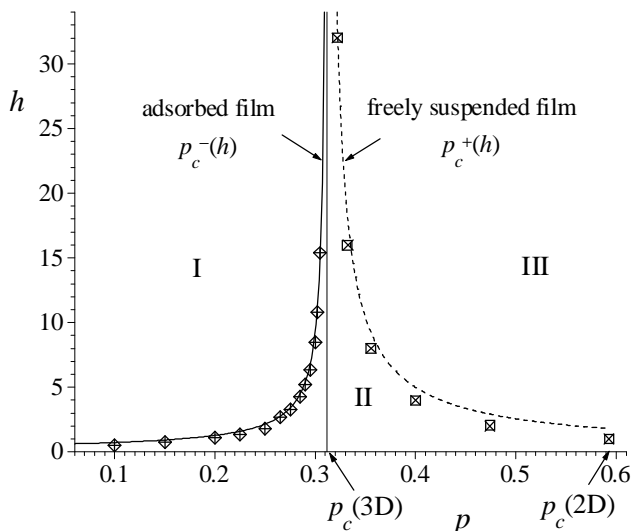


FIG. 8: Diagram of the percolation thresholds $p_c^-(h)$ and $p_c^+(h)$ as a function of the film thickness h . $p_c^-(h)$ is the percolation threshold in an adsorbed film. It is defined here as the ensemble of points for which $\zeta^{3D}(p) \equiv h$. Diamonds symbols correspond to the same data set as in Fig. 7. The continuous line is the fit with equation 56. $p_c^+(h)$ is the percolation threshold in a freely suspended film. Square symbols corresponds to the data in Fig 5. The dashed line is the fit with eq. (52) in section IV.

The curve $p_c^+(h)$ is defined by eq. 52. It corresponds to the percolation threshold in the direction parallel to the film. Note that it corresponds also to the glass transition in a freely suspended film of thickness h , as defined in Section IV. The two curves $p_c^-(h)$ and $p_c^+(h)$ define 3 regions in the plane (p, h) . In region I, one has $\zeta < h < d$. Clusters connecting both faces of a film of thickness h are exponentially rare. In Region III, there is an infinite cluster extending throughout a film of thickness h . Region II corresponds to intermediate cases $h < \zeta < d$. For a given thickness h , this corresponds to going from $p_c^+(h)$ to $p_c^-(h)$ within region II. In this region, some clusters have a lateral extension large with respect to h . As one comes closer to the curve $p_c^+(h)$, the correlation length parallel to the plane of the film, i.e. the lateral extension of clusters ζ diverges. One can see such an aggregate in Fig. 9. Thus, in this section, we study the distribution of cluster sizes and masses, both on the surface and in the bulk of a film of thickness h . The corresponding results are of interest for describing the cross-over between freely suspended films and strongly adsorbed films as far as glass transition is concerned [30].

We will check that the distribution of clusters and their structure may be described by the procedure detailed in Section II C, in which we assumed that a percolation system of thickness h may be renormalized to a true 2D system by coarse-graining at the scale h . Note that the system has to be larger than the typical lateral extension of large clusters, which become larger as one comes closer to $p_c^+(h)$. On the other hand, the second moment of the

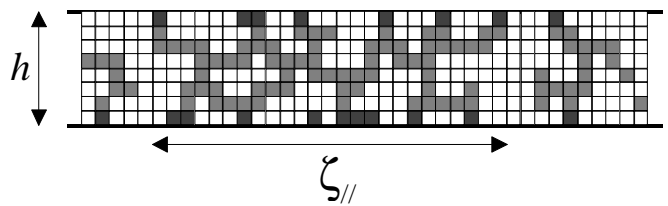


FIG. 9: Schematics of a cluster percolating through the film thickness, in the regime $h < \zeta < d$. The 'surface mass' s of the cluster is given by the ensemble of sites at the surface of the film, which are emphasized.

distribution of cluster masses $n(s)$ is dominated by the contribution from large clusters, which are exponentially rare. Thus, we need here to simulate both large enough systems and a large enough number of realisations of a given system, which is quite demanding in terms of computer size and time. The volume $V = h \times d^2$ of the simulated systems is of the order a few 10^8 typically. Results are averaged over 20 to 50 different realisations, depending on the distance to the $p_c^+(h)$ curve.

A. The average mass of the clusters

Let us consider a cluster in a film of thickness h , in the regime $h < \zeta < d$ (i.e. in Region II of the diagram in Fig. 8). It was shown in Section II C how a film of thickness h may be renormalized to a 2D percolation system. Specifically, in the regime $h < \zeta < d$, the average mass M , expressed in units of elementary sites and defined as in eq. (4), is given by eq. (35), i.e.:

$$M(h, p) = M_0 h^{2-\eta_3} \left(h^{1/\nu_3} |p - p_c(h)| \right)^{-\gamma_2} \quad (57)$$

The 2D behaviour is reflected in the exponent $-\gamma_2$. We have obtained the distribution of cluster masses $n(m)$ for different values of p and h (within region II) in systems of total volume of the order 2.6×10^8 , and computed the second moment $M(h, p)$ (see eq. (4)).

Let us first consider the variation versus p , h being fixed. For each value of h , the variation of $M(h, p)$ versus $p_c(h) - p$ gives a power law with the exponent $-\gamma_2 = -2.389$ in the limit p close to $p_c(h)$, in agreement with the expected behaviour. To illustrate this power law and the influence of the thickness h of the system, the curves $M(h, p)$ are plotted as a function of the quantity $X = h^{1/\nu_3}(p_c(h) - p)$ in Fig. 10a for different values of h . The values at $\log X = 0$ for each portion of curve in Fig. 10 (corresponding to a given value of h) gives the prefactor $M_0(h)$ in the curves $M(p, h)$ versus X . In the limit of large h , the behaviour of the prefactor $M_0(h)$ is compatible with a power law $M_0(h) = M_0 h^{2-\eta_3}$ ($2 - \eta_3 = 2.068$). The prefactor M_0 has the value $M_0 \approx 0.233$.

The quantity $M' = h^{-2+\eta_3} M(h, p)$ plotted versus X should then give a master curve of the form $M' =$

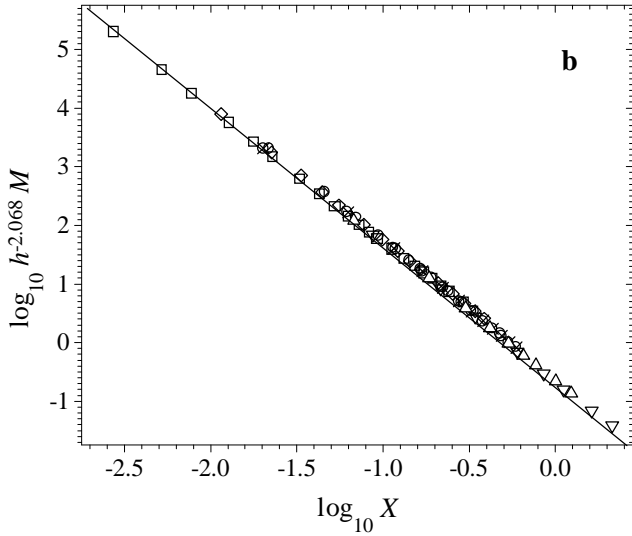
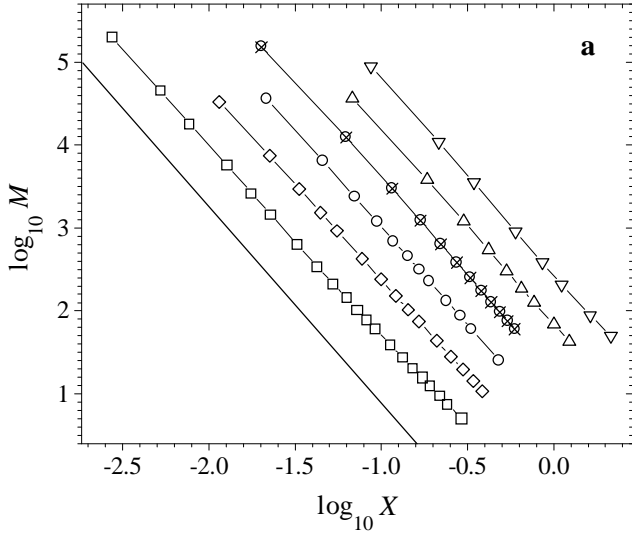


FIG. 10: **a**: the average mass $M(h, p)$ vs $X = h^{1/\nu_3} (p_c(h) - p)$, **b**: the quantity $M' = h^{-2+\eta_3} M(h, p)$ vs X , for different values of h : \square : $h = 1$, \diamond : $h = 2$, \circ : $h = 4$, \otimes : $h = 8$, \triangle : $h = 16$, ∇ : $h = 32$. The straight lines corresponds to the exponent $-\gamma_2 = 43/18 = 2.389$. In **b**, a master curve is obtained to an excellent approximation.

$M'_0 X^{-\gamma_2}$. This is illustrated in Fig. 10b. The expected behaviour is indeed observed to an excellent approximation in a large range of variation (more than 4 decades in M). The full scaling behaviour of $M(h, p)$ as a function of $p_c(h) - p$ and h (eq. (57)) is thus summarized in Fig. 10b. Remember that M' represents the mass expressed in number of renormalized supersites. Alternatively, the same work may be done with the surface mass s of the clusters, i.e. the number of sites belonging to a cluster which are in contact with the substrate (the surface mass of clusters is denoted by s in order to distinguish it from their total mass m . See Fig. 9). The average surface mass was obtained in the following way. The distribution $n(s)$,

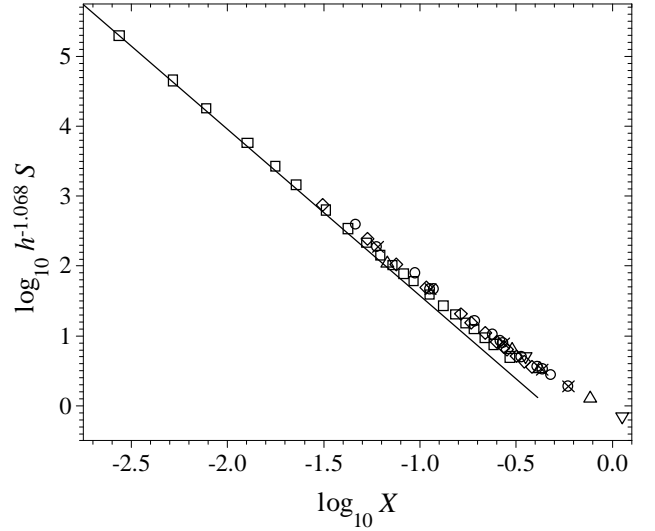


FIG. 11: The reduced average surface mass $h^{-1+\eta_3} S(h, p)$ vs the quantity $X = h^{1/\nu_3} (p_c(h) - p)$ in log scale, for different values of the thickness h . The straight line corresponds to the exponent $-\gamma_2 = 43/18 = 2.389$.

which gives the number of clusters with a surface mass s , was recorded for different values of h and p (in region II of the diagram in Fig. 8). The average surface mass $S(p, h)$ was then computed as the second moment:

$$S(h, p) = \frac{\sum s^2 n(s)}{\sum s n(s)} \quad (58)$$

where the summation extends over all clusters which percolate through the film thickness.

In a way similar to $M(h, p)$, $S(h, p)$ is expected to scale like:

$$S(h, p) = S_0 h^{1-\eta_3} \left(h^{1/\nu_3} |p - p_c(h)| \right)^{-\gamma_2} \quad (59)$$

When plotted versus $(p - p_c(h))$, for each value of h , $S(h, p)$ gives a power law with the exponent $-\gamma_2 = -2.389$, in agreement with the expected behaviour and with the behaviour observed for the quantity $M(p, h)$. From eq. (59), a master curve should be obtained when the quantity $h^{\eta_3-1} S(h, p)$ is plotted versus $X = h^{1/\nu_3} (p_c(h) - p)$. This is shown in Fig. 11. Here also, the expected asymptotic behaviour is observed to an excellent approximation in a large range of variation for S . The prefactor S_0 has the value $S_0 \approx 0.24$.

B. The distribution of cluster masses in the surface of the film

In this Section, we show that not only the average mass, but also the whole distribution of cluster masses obeys scaling laws in the two variables h and $p - p_c(h)$, which allows to draw a master curve. According to

Eq. (43), the number of clusters of mass m obeys (in the limit of large m):

$$h^{-\omega} m^{\tau_2} n(m) \approx g_{2D} \left[h^{-D_3+1/\sigma_2\nu_3} |p - p_c(h)|^{1/\sigma_2} m \right] \quad (60)$$

i.e., the quantity $h^{-\omega} m^{\tau_2} n(m)$ should give a master curve when plotted versus the quantity $h^{-D_3+1/\sigma_2\nu_3} |p - p_c(h)|^{1/\sigma_2} m$. The characteristic exponents of h have the values $-D_3 + 1/\sigma_2\nu_3 = 0.342$ and $\omega = -0.323$. Consider first the variation versus $p - p_c(h)$, h being fixed. The distributions of clusters, represented by the quantity $m^{\tau_2} n(m)$, obtained for $h = 4$ and different values of $p - p_c(h)$, are plotted as a function of m in Fig. 12a. For each value of h ($h = 1$ to $h = 32$), an excellent superposition property is observed when $m^{\tau_2} n(m)$ is plotted as a function of the reduced variable $|p - p_c(h)|^{1/\sigma_2} m$. This is illustrated in Fig. 12b, in which the various curves shown in Fig. 12a ($h = 4$) are superposed.

Two exponents have to be adjusted in order to superpose the ensembles of curves obtained for different values of h . First, plotting the quantity $\log m^{\tau_2} n(m)$ as a function of the reduced variable $h^{-D_3+1/\sigma_2\nu_3} |p - p_c(h)|^{1/\sigma_2} m$ allows the slopes obtained in the asymptotic limit at large m to coincide. Then, the quantity $\log h^{-\omega} m^{\tau_2} n(m)$ is plotted as a function of the reduced variable $h^{-D_3+1/\sigma_2\nu_3} |p - p_c(h)|^{1/\sigma_2} m$. This procedure is illustrated in Fig. 12c. As mentioned above, according to eq. 60, a master curve should be obtained.

The quantity $\log h^{-\omega} m^{\tau_2} n(m)$ does indeed show a linear asymptotic behaviour at large m values, i.e. for clusters larger than the correlation length ζ . It is observed in Fig. 12c that the slopes obtained at large m values indeed coincide, within numerical uncertainties. In contrast, vertical superposition of the curves obtained for various h values is only observed asymptotically, i.e. towards the largest investigated value $h = 32$. The large dispersion in the curves comes from the numerical limitations of the present simulations, especially for large values of h and/or $p_c(h) - p$. In this regime, where the correlation length ζ is large, the lateral size d of the system has to be large, and the distributions $n(m)$ extend towards large m values. As already mentioned, computing the distributions $n(m)$ with a good sampling of large m values is very demanding in terms of memory size and computer time. In any case, it can be concluded at this point that our data are compatible with the scaling law in eq. 60 in the asymptotic regime of large h values, which is particularly clear when considering the data corresponding to the thicknesses $h = 8, 16$ and 32 respectively.

To illustrate further the scaling properties expressed in eq.(60), we have fitted the exponential decrease of $m^{\tau_2} n(m)$ at large m values. This procedure gives the quantity $m_\zeta(p, h)$, which depends on p and h and may be considered also as a typical mass describing the distribution of the clusters within the film (see eq.(2)). From

eq.(60), m_ζ obeys the following scaling law:

$$m_\zeta \approx h^{D_3} \left[h^{1/\nu_3} |p - p_c(h)| \right]^{-1/\sigma_2} \quad (61)$$

First, for each value of h , it is observed that $m_\zeta(p, h)$ follows a scaling law when plotted as a function of $(p - p_c(h))$, with the exponent $-1/\sigma_2 = -2.528$. Then a master curve is obtained when $h^{-D_3} m_\zeta(p, h)$ is plotted as a function of the quantity $h^{1/\nu_3} (p - p_c(h))$. The obtained master curve is shown in Fig. 13.

C. The structure of the clusters in a film of thickness h

The structure of the clusters is described by the relationship between the mass m of a cluster (the number of sites belonging to the cluster) and its size r . Clusters have a fractal structure characterized by the exponent D defined as $r \approx m^{1/D}$, in which the value of D effectively measured varies according to the location of the system with respect to p_c , or equivalently, according to the typical range of sizes which is probed compared to the correlation length $\zeta(p)$ (see eq. (17) and the discussion thereafter). The cluster size may be defined as either the gyration radius or some measure of the cluster extension.

We have studied the relationship between the size and mass of clusters in a film of thickness h , within the interval $p_c^-(h) < p < p_c^+(h)$. The squared size of a cluster i is defined here as $r_i^2 = \Delta x_i^2 + \Delta y_i^2$, where Δx_i and Δy_i are the maximum extensions of the cluster i along x and y (x and y are the coordinates parallel to the plane of the film), or more precisely, the maximum extensions of the intersection of the cluster with the limiting surfaces of the film. The mass m_i is the total number of sites which belong to cluster i (within the whole volume of the film). The quantity r_i^2 is then averaged over all clusters of mass m , in order to obtain the squared average size $\overline{r^2}(m)$ as a function of m :

$$\overline{r^2}(m) = \frac{1}{Vn(m)} \sum_i r_i^2 \quad (62)$$

where the sum is extended over the $Vn(m)$ clusters having the mass m ($V = d^2 \times h$ is the volume of the system). The relationship between the mass m and the average size $R = (\overline{r^2}(m))^{1/2}$ of the clusters in a film of variable thickness h is illustrated in Fig. 14.

Some examples of the curves $R(m)$, obtained in a system of lateral dimension $d = 2048$ and different values of the thickness h (from $h = 1$ to $h = 16$) are plotted in logarithmic scale in Fig. 14, for an occupation probability $p = 0.315$. The observations which can be made on Fig. 14 are the following. First, two different regimes are observed. They are characterised by well defined power laws, with different exponents. At small R values (typically, R smaller than or of the order of h), the mass grows

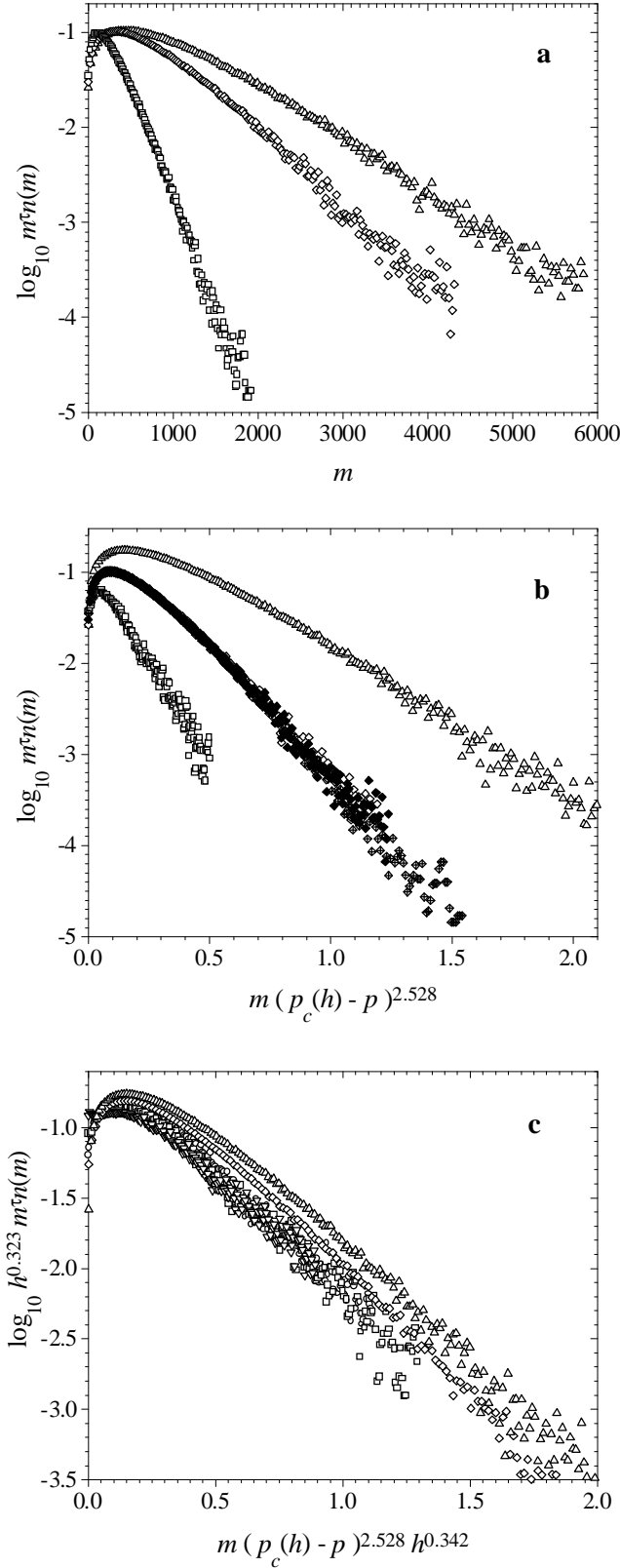


FIG. 12: Scaling properties of the distribution $m^{\tau_2} n(m)$, where $n(m)$ is the number of clusters of mass m per lattice site. a: $\log m^{\tau_2} n(m)$ plotted versus m for a thickness $h = 4$ and different values of the occupation probability p : \square : $p = 0.34$, \diamond : $p = 0.36$, \triangle : $p = 0.365$. b: $\log m^{\tau_2} n(m)$ plotted versus $|p - p_c(h)|^{1/\sigma_2} m$, for different values of h : \triangle : $h = 1$, \diamond and \blacklozenge : $h = 4$, \square : $h = 16$. In this representation, the curves obtained for different values of p at fixed h superpose. c: $h^{-\omega} \log m^{\tau_2} n(m)$ plotted versus the quantity $h^{0.342} |p - p_c(h)|^{1/\sigma_2} m$, for different values of p and h : \triangle : $p = 0.54$, $h = 1$, \diamond : $p = 0.34$, $h = 4$, \circ : $p = 0.34$, $h = 8$, \square : $p = 0.32$, $h = 16$, ∇ : $p = 0.31$, $h = 32$. The curves

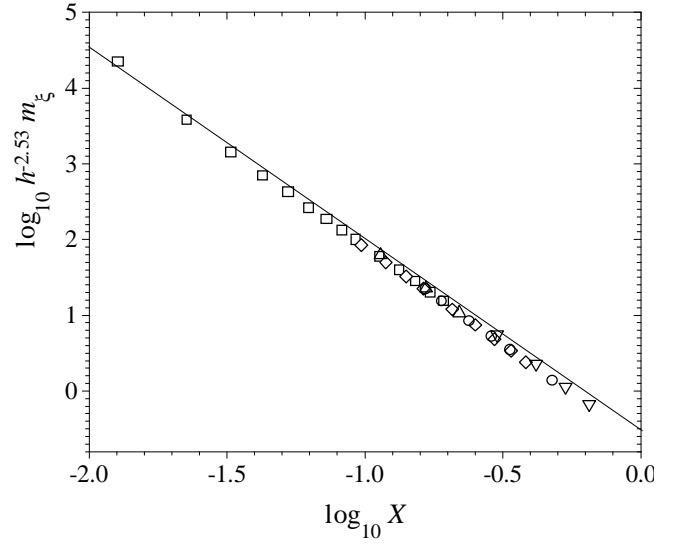


FIG. 13: The quantity m_{ξ} obtained by fitting the distribution $m^{\tau_2} n(m)$ at large m . The quantity $h^{-D_3} m_{\xi}$ is plotted versus $X = h^{1/\nu_3} (p - p_c(h))$, for different values of h : \square : $h = 1$, \diamond : $h = 2$, \circ : $h = 4$, \triangle : $h = 8$, ∇ : $h = 16$. A master curve is obtained to an excellent approximation. The straight line corresponds to the exponent $-1/\sigma_3 = -2.528$.

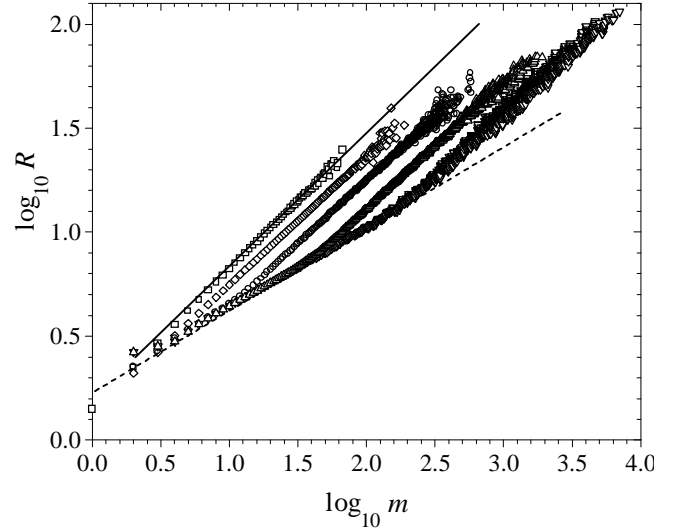


FIG. 14: The average lateral size $R = (\overline{\Delta x^2 + \Delta Y^2})^{1/2}$ is plotted as a function of the total mass m of the clusters, in films of various thickness h : \square : $h = 1$, \diamond : $h = 2$, \circ : $h = 4$, \triangle : $h = 8$, ∇ : $h = 16$. The occupation probability $p = 0.315$. The straight lines have a slope $1/1.561$, which corresponds to the fractal exponent $D_2 = 1.56$ at $p < p_c$.

with R faster than for larger R values. Indeed, clusters should behave in a 3D way in this regime. Within the whole interval $p_c^-(h) < p < p_c^+(h)$, the 3D correlation length is larger than h . Thus, the expected behaviour in this regime should be described by the fractal exponent $1/D_3$ at p_c^{3D} , according to eq. (17) and the discussion

thereafter. This is indeed the case: the slope of this part of the curves is compatible with the value $1/D_3 = 0.395$ at $p = p_c^{3D}$. This regime is illustrated by the dashed line in Fig. 14. Then, at $R \approx h$, each curve has a crossover to another regime. For $R > h$, one enters a quasi 2D regime, in which the correlation length in the equivalent (renormalized) 2D system is small. Therefore, the slope in this regime has to be compared to the value of the fractal exponent at $p < p_c^{2D}$: $1/D_2^< = 0.641$ [1]. This quasi 2D regime is illustrated by the solid line in Fig. 14. The observed behaviour is indeed compatible with the exponent $1/D_2^<$.

Thus, the results in Fig. 14 illustrates the quasi 2D behaviour of the film: a film of thickness h behaves as a strictly 2D film. In the equivalent renormalized 2D system, the 2D scaling law, eq. 16, writes:

$$m' = m_0 R'^{D_2^<} \quad (63)$$

where m_0 is a prefactor of order unity (the superscript $<$ indicates that the exponent $D_2^<$ is that at $p < p_c^{2D}$). Coming back to the original system of thickness h , the size (expressed in units of elementary sites) becomes $R' \rightarrow R = hR'$ and the mass is transformed as $m' \rightarrow m = h^{D_3} m'$, since $\zeta_{3D} > h$. Eq. (63) thus leads to the following scaling:

$$m = m_0 h^{D_3} \left(\frac{R}{h} \right)^{D_2^<} \quad (64)$$

From the data in Fig. 14, the value of the prefactor $m_0 \approx 0.22$. Close inspection of the data in Fig. 14 shows however that the apparent exponent in the regime $R > h$ is slightly smaller than $1/D_2^<$ in some range of R values at the beginning of this regime. Indeed, the scaling $m' \approx R'^{D_2^<}$ is only valid when $R > \zeta_{||}$, where $\zeta_{||}$ is the correlation length parallel to the film. In the range $h < R < \zeta_{||}$, one should observe a power law $m \propto R^{1/D_2}$ where $1/D_2 = 49/91 \approx 0.538$ is the critical exponent at p_c . It just happens here that the range is too small for this regime to be clearly visible. For instance, $\zeta_{||}$ (expressed in units of h -cubes) is:

$$\zeta_{||} \approx \zeta_0 \left(h^{1/\nu_3} |p_c^+(h) - p| \right)^{-\nu_2} \quad (65)$$

which gives for the particular case of the data shown in Fig. 14, a value $\zeta_{||} \approx 3.2$ (with a prefactor ζ_0 of the order 1).

VII. CONCLUSION

We have described here the cross-over between 2D and 3D percolation. This work demonstrates that a system of finite thickness h may be renormalized to a strictly 2D system for describing the percolation properties, provided that the 2D percolation threshold p_c^{2D} is renormalized to an appropriate value $p_c(h)$. The values $p_c(h)$ have been determined numerically with a good precision for $h = 2$ to $h = 128$ (see Table III), in the case of a cubic lattice. We have studied 3 different regimes, which describe 3 different physical situations. These regimes are represented in Fig. 8. At a given value of the occupation probability p , if the thickness h is larger than the 3D correlation length, the problem is a true 3D problem. The fraction of sites of one interface connected to the other interface by a cluster is exponentially small. The corresponding correlation function and correlation length are given by 3D critical exponents. Our numerical simulations provide the corresponding pre-factors. If, at a given value of p , the thickness h is smaller than the 3D correlation length, then the problem is equivalent to a 2D problem. We provide the corresponding transformations for calculating the correlation length parallel to the film, the average mass of the clusters and the cluster mass distribution, among other relations. These quantities can be expressed as functions of known 2D and 3D critical exponents. Our numerical simulations provide the corresponding pre-factors for these quantities, as well as the master function for the mass distribution. These results can be used for describing the glass transition in thin polymer films as described in [30], and should be also of interest for describing mechanical or electrical properties of films made of composite and disordered materials.

-
- [1] Stauffer D. and Aharony A., *Introduction to percolation theory* (Taylor and Francis, London) 1994
- [2] Stauffer D., *Phys. Rep.*, **54** (1979) 1
- [3] Sahimi M., *Applications of percolation theory* (Taylor and Francis, London) 1994
- [4] Essam J.W., *Rep.Prog.Phys.*, **43** (1980) 833
- [5] De Gennes P.-G., *Scaling Concepts in Polymer Physics* (Cornell University Press, Ithaca) 1986
- [6] Obukhov S.P., *Phys. Rev. Lett.*, **74** (1995) 4472
- [7] Alexander S., *Phys. Rep.* **296** (1998) 65
- [8] Domb C. and Lebowitz J.L. Editors, *Phase Transitions and Critical Phenomena* **8** (Academic Press, London) 1983: Chapter 1 by Binder K. and Chapter 2 by Barber M.N.
- [9] J.P. Clerc J.P., Giraud G., Alexander S. and Guyon E. *Phys. Rev. B* **22**, (1980) 2489
- [10] Vicsek T. and Kertész J., *Phys. Lett.*, **81A** (1981) 51
- [11] Ediger M.D., Angell C.A. and Nagel S.R., *J.Phys.Chem.* **100** (1996) 13200
- [12] *Review articles in Science*, **267** (1995) 1924
- [13] Schmidt-Rohr K. and Spiess H.W., *Phys. Rev. Lett.*, **66** (1991) 3020

- [14] Heuer A., Wilhelm M., Zimmermann H. and Spiess H.W., *Phys. Rev. Lett.*, **75** (1995) 2851
- [15] Tracht U., Wilhelm M., Heuer A., Feng H., Schmidt-Rohr K. and Spiess H.W., *Phys. Rev. Lett.*, **81** (1998) 2727
- [16] Cicerone M.T., Blackburn F.R. and Ediger M.D., *Macromolecules*, **28** (1995) 8224
- [17] Wang C.-Y. and Ediger M.D., *J. Chem. Phys.*, **112** (2000) 6933
- [18] Sillescu H., *J. Non-Cryst. Solids*, **243** (1999) 81
- [19] Ediger M.D., *Annu. Rev. Chem.*, **51** (2000) 99
- [20] Richert R., *J. Phys.: Condens. Matter*, **14** (2002) R703
- [21] Long D. and Lequeux F., *EPJ E*, **4** (2001) 371
- [22] Merabia S. and Long D., *EPJ E*, **9** (2002) 195
- [23] Keddie J.L., Jones R.A.L., and Cory R.A., *Europhys. Lett.*, **27** (1994) 59
- [24] Kawana S. and Jones R.A.L., *Phys. Rev. E.*, **63** (2001) 021501
- [25] Wallace W.E., van Zanten, J.H. and Wu W.L., *Phys.Rev.E.*, **52** (1995) R3329
- [26] Grohens Y., Brogly M., Labbe C., David M.-O. and Schultz J., *Langmuir*, **14** (1998) 2929
- [27] Carriere P., Grohens Y., Spevacek J. and Schultz J., *Langmuir*, **16** (2000) 5051
- [28] Forrest J.A. and Dalnoki-Veress K., *Adv. Colloid Interfac. Sci.*, **94** (2001) 167
- [29] Forrest J.A., *EPJ E*, **8** (2002) 261
- [30] Long D. and Sotta P., submitted (2002)
- [31] Fryer D.S., Peters E.J., Kim J.E., Tomaszewski J.E., de Pablo J.J., Nealey P.F., White C.C. and Wu W., *Macromolecules* **34** (2001) 5627
- [32] Pham J.Q. and Green P.F., *J. Chem. Phys.* **116** (2002) 5801
- [33] Hoshen J. and Kopelman R., *Phys. Rev. B*, **14** (1976) 3428